Clays and Clay Minerals, Vol. 31, No. 3, 207–217, 1983.

ACTIVITY/COMPOSITION RELATIONS AMONG SILICATES AND AQUEOUS SOLUTIONS: II. CHEMICAL AND THERMODYNAMIC CONSEQUENCES OF IDEAL MIXING OF ATOMS ON HOMOLOGICAL SITES IN MONTMORILLONITES, ILLITES, AND MIXED-LAYER CLAYS

PER AAGAARD[1] AND HAROLD C. HELGESON

Department of Geology and Geophysics, University of California
Berkeley, California 94720

Abstract—The activities of thermodynamic components of clay minerals corresponding in composition to pyrophyllite, muscovite, paragonite, and margarite were computed from chemical analyses reported in the literature assuming ideal mixing of atoms on homological sites in the minerals. These activities were then used to generate stability fields for smectites, illites, and mixed-layer clays on logarithmic activity diagrams representing equilibrium among minerals and aqueous solutions at 25°C and 1 bar. Comparative analysis indicates that the approach affords close approximation of both mineral and water compositions in geologic systems.

Key Words—Activity, Atom mixing, Illite, Mixed layers, Montmorillonite, Thermodynamics.

INTRODUCTION

Logarithmic activity diagrams have been used extensively to interpret the chemistry of aqueous solutions coexisting with mineral assemblages in geologic environments. However, nonstoichiometric minerals such as illite and montmorillonite are commonly represented in these diagrams by either hypothetical end members or pseudostoichiometric analogs of natural solid solutions with specified compositions and discrete, standard molal Gibbs free energies of formation. The idealized stoichiometry assigned to these minerals dictates the intercepts and slopes of their stability field boundaries on activity diagrams, but the compositions of the minerals rarely coincide with those of their natural counterparts. As a consequence, the diagrams may be both unrealistic and misleading.

Although standard molal Gibbs free energies of formation from the elements for nonstoichiometric minerals with specified compositions have been measured experimentally (e.g., Kittrick, 1971; Routson and Kittrick, 1971) and estimated from cation-exchange data, water compositions, and corresponding states algorithms (e.g., Helgeson, 1969; Tardy and Garrels, 1974; Nriagu, 1975; Mattigod and Sposito, 1978; Merino and Ransom, 1982), they are hardly representative of the wide spectrum of mineral compositions observed in nature, and in many instances their reliability is open to serious question. For example, R. M. Garrels (Department of Marine Science, University of South Florida, St. Petersburg, Florida, written communication, 1982) calculates that if an ideal solid solution consisting of 50 mole percent each of components designated by AX and BX dissolves in H_2O until it reaches stoichiometric saturation, and if the equilibrium constants for $AX = A^+ + X^-$ and $BX = B^+ + X^-$ differ by two orders of magnitude, the absolute error associated with assuming that equilibrium has been achieved between $A_{0.5}B_{0.5}X$ and the aqueous phase is of the order of 2.5 kcal/mole.

The limited utility of assigning standard molal Gibbs free energies of formation to solid solutions with given compositions is underscored by the fact that it would take an enormous number of such data to represent adequately the thermodynamic behavior of minerals of variable composition in geochemical processes. In contrast, mixing equations which take explicit account of both independent and coupled compositional variation on tetrahedral, octahedral, and exchange sites in minerals afford generality and allow accurate depiction on two-dimensional activity diagrams of the relative stabilities of naturally occurring multi-component minerals of highly variable composition (Helgeson and Aagaard, 1984). The purpose of the present communication is to demonstrate the advantages of this approach by generating activity diagrams with the aid of random mixing approximations for equal interaction of cations on equivalent structural sites in illites, montmorillonites, and mixed-layer clays.

MIXED-LAYER CLAYS

Considerable evidence has accumulated in recent years suggesting that mixed-layer clays are not continuous solid solutions, but mixtures of dioctahedral phases, which themselves may exhibit only slight compositional variation. Perhaps the most compelling evidence

[1] Present address: Institute of Geology, University of Oslo, Oslo 3, Norway.

https://doi.org/10.1346/CCMN.1983.0310306 Published online by Cambridge University Press

of this kind can be adduced by comparing the distribution and character of authigenic illite and smectite in sandstones and shales. Discrete grains of authigenic illite and smectite (which may or may not contain illite interlayers) commonly occur in sandstones, where the illite bridges pore spaces and the smectite lines the walls of the pores (Wilson and Pittman, 1977; Welton, 1980). In contrast, authigenic illite and smectite are intimately interlayered in shales, which exhibit random intrastratification ranging from ~35 to 100% montmorillonite (Reynolds and Hower, 1970; Perry and Hower, 1970). With increasing depth and temperature, the smectite interlayers react with K-feldspar and/or muscovite to produce progressively more illitic mixed-layer clays (Perry and Hower, 1970; Hower *et al.*, 1976). Under certain circumstances, extensive solid solution may occur in the smectite layers of mixed-layer clays, which may or may not be related to solid solution in the illitic layers (Velde, 1977). The discrete distribution, and particularly the selective reaction of the smectite interlayers on a scale of tens of Ångstrom units in shales suggest that at least in these cases the mixed-layer clays behave as mixtures of phases, rather than solid solutions.

Despite the fact that the field and laboratory evidence adduced above indicate that mixed-layer clays commonly behave as polyphase aggregates, under other circumstances they may behave as solid solutions (Zen, 1962; Velde, 1977). For example, the latter behavior might occur in the absence of K-feldspar or K-mica (see above) if the smectite and illite interlayers exhibit a homogeneous distribution with a stacking periodicity of the order of 10–50 Å or less. Because ultrafine interlayering on the scale of unit-cell dimensions is common in both shales and hydrothermal alteration zones (Page, 1977; Sudo *et al.*, 1981), it seems desirable to explore the thermodynamic consequences of compositional variation in clay minerals by first treating mixed-layer clays as though they behave as solid solutions. The solid solution model can then be compared with the thermodynamic consequences of regarding mixed-layer clays as polyphase aggregates to determine which approach better describes the behavior of the clays in geochemical processes.

Truesdell and Christ (1968) and Stoessell (1979, 1981) adopted regular solution models to calculate the thermodynamic consequences of compositional variation in montmorillonites and illites, respectively. In contrast, Helgeson and MacKenzie (1970) and Tardy and Fritz (1981) regarded clay minerals as ideal solutions of thermodynamic components. An alternate frame of reference can be established to calculate the thermodynamic properties of clay minerals by assuming ideal mixing of atoms on equivalent structural sites in the minerals, which is the approach taken below. Local equilibrium constraints imposed by immiscibility in mixed-layer clays will be the subject of a subsequent communication.

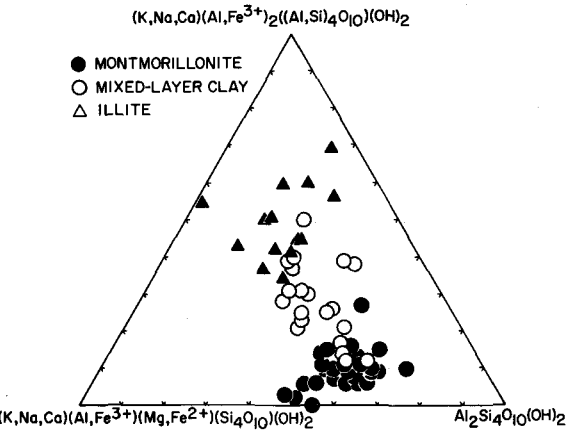

Figure 1. Compositions of clay minerals considered in the present study. The symbols represent data reported by Hower and Mowatt (1966), Schultz (1969), and Weaver and Pollard (1973).

COMPOSITIONAL VARIATION AND SUBSTITUTIONAL ORDER/DISORDER IN CLAY MINERALS

The thermodynamic consequences of preferential site occupancy and mixing of atoms on crystallographic sites in clay minerals can be assessed by first computing site populations from chemical analyses of naturally occurring clay minerals reported in the literature (see below). A number of clay mineral compositions are shown in Figure 1. For the most part the three types of clay minerals shown in the figure exhibit relatively discrete compositional ranges which are contiguous in the sequence montmorillonite, mixed-layer clay, illite. Although the continuity of this sequence is not diagnostic with respect to whether mixed-layer clays consist of one or more phases (Zen, 1962), montmorillonites, mixed-layer clays, and illites can be regarded for the purpose of demonstrating the consequences of ideal mixing of atoms on homological sites in clay minerals as members of a continuous solid solution series.

Mössbauer data for illites and montmorillonites (Coey, 1975; Ericsson *et al.*, 1977) indicate that in most dioctahedral clay minerals formed at or near 25°C the tetrahedral layers are completely disordered. X-ray powder and electron diffraction data indicate that the aluminum-oxygen and silicon-oxygen bond lengths in 2*M* mica components other than margarite, which exhibits complete tetrahedral order consistent with the aluminum avoidance principle (Guggenheim and Bailey, 1975), are all essentially equivalent (Zvyagin, 1967; Burnham and Radoslovich, 1964). This observation suggests nearly complete tetrahedral disorder. Gatineau's (1964) arguments in favor of short-range tetrahedral order in layer silicates lead to inconsistencies with the aluminum avoidance principle. In addition, the ideal space groups of the 1*M* polytypes rule out tetrahedral order in celadonite and other 1*M* mica components.

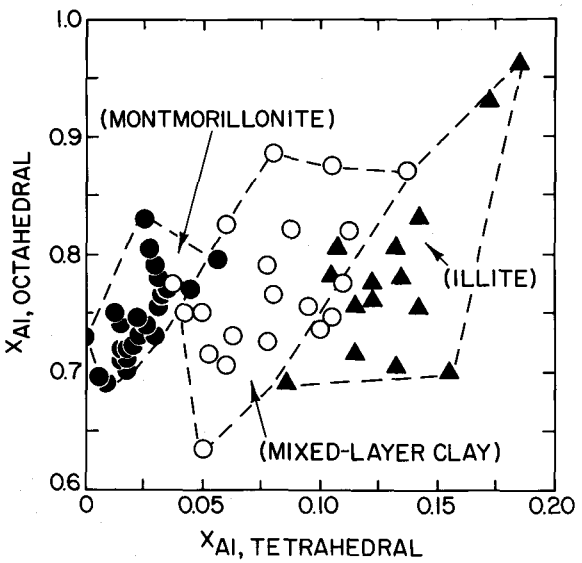

Figure 2. Site occupancy of aluminum in the clay minerals shown in Figure 1. The dashed lines designate limiting values of $X_{Al,Tetrahedral}$ and $X_{Al,Octahedral}$ defined by the distribution of the data for illites, montmorillonites, and mixed-layer clays (see text).

The observations summarized above are consistent with conclusions reached from structure refinements of layer silicates by Smith and Yoder (1956), Zvyagin (1967), and others. Although Bailey (1975) questioned the validity of using ideal space groups in these structure refinements (and suggested that tetrahedral order may be more prevalent than previous studies indicate), it nevertheless appears reasonable to assume on the basis of all the various data currently available that in most cases tetrahedral disorder prevails in low-temperature layer silicates other than margarite and rare polytypes such as phengite $2M_2$ and muscovite $3T$. This assumption is consistent with relatively rapid formation of the layer silicates in a metastable state of disorder.

Mössbauer data and structure refinements indicate that of the three octahedral sites in layer silicates, the M(2) sites are homological, or nearly so. The M(1) sites are essentially vacant in the dioctahedral micas, but the M(2) sites in these minerals are completely filled. Relatively few spectral and/or structural data are available for clay minerals which can be used to calculate unambiguously site occupancies in montmorillonites, illites, and mixed-layer clays. As a consequence, site occupancies must usually be estimated from compositional data and idealized structural formulae. Site occupancies in the clay minerals considered in the present study were taken from Hower and Mowatt (1966), Schultz (1969), and Weaver and Pollard (1973), who calculated the distribution of atoms among the exchange, octahedral, and tetrahedral sites from analytical data using the equations and approach summarized by Ross and Hendricks (1945) and Brown and Norrish (1952). Independently determined cation-exchange capacities were taken into account in the calculations of exchange-site occupancies. In this way, ambiguities in the total site occupancy of the octahedral and tetrahedral layers (Hower and Mowatt, 1966) were minimized. Although a recent Mössbauer study of clay minerals indicates that Fe^{3+} may enter into tetrahedral coordination in montmorillonite (Ericsson *et al.*, 1977), all Fe^{3+} was assigned by Hower and Mowatt (1966), Schultz (1969), and Weaver and Pollard (1973) to the octahedral layers. Errors arising from omitting provision for tetrahedral Fe^{3+} introduce negligible uncertainties in the calculations presented below. Similarly, discrepancies introduced by slight partitioning of Fe^{3+} on the M(1) sites in montmorillonite (Ericsson *et al.*, 1977) have only a minor effect on the thermodynamic behavior of the mineral.

Several criteria were used in the present study to select the most reliable computed site populations from among the many reported in the literature. Only those samples for which the weight percent of both FeO and Fe_2O_3 are given were accepted, and of these, only those for which the weight percent oxides sum to 100 ± 3 were considered sufficiently well characterized for thermodynamic analysis. Total octahedral occupancy per gram formula unit was restricted to a range of 1.9 to 2.1 for illites and 1.95 to 2.05 for montmorillonites and mixed-layer clays. Illites were distinguished from montmorillonites and mixed-layer clays according to the percent expandable layers, which was taken to be <10 for illites, 10–65 for mixed-layer clays, and >65 for montmorillonites. The cation-exchange capacities of the montmorillonites considered in the present study are >90 meq/100 g.

Of the samples for which site occupancies were computed by Hower and Mowatt (1966), Schultz (1969), and Weaver and Pollard (1973), 65 "representative" clay minerals met the criteria summarized above. These consist of 15 illites, 30 montmorillonites, and 20 illite/montmorillonite mixed-layer clays from a variety of geologic formations in various parts of the world ranging in age from the Paleozoic to Recent. Nevertheless, it can be seen in Figure 2 that all of the dioctahedral clay minerals can be characterized by assessing the distribution of Al^{3+} among the octahedral and tetrahedral sites. Note that tetrahedral site occupancy alone suffices to distinguish unambiguously montmorillonites from illites. Distinctions of this kind are also manifested by the activities of the thermodynamic components of clay minerals.

CALCULATION OF THE ACTIVITIES OF THE THERMODYNAMIC COMPONENTS OF CLAY MINERALS

The activity of the ith thermodynamic component of a solid solution (a_i) can be computed from (Helgeson and Aagaard, 1984)

https://doi.org/10.1346/CCMN.1983.0310306 Published online by Cambridge University Press

$$a_i = \mathbf{k}_i \prod_s \prod_j a_{j,s}^{\nu_{s,j,i}} = \mathbf{k}_i \prod_s \prod_j (X_{j,s}\lambda_{j,s})^{\nu_{s,j,i}}, \quad (1)$$

where $\mathbf{k}_i$ represents a constant relating the inter- and intracrystalline standard states for the ith component (which may be temperature and/or pressure dependent), $a_{j,s}$, $\lambda_{j,s}$, and $X_{j,s}$ stand for the activity, activity coefficient, and mole fraction of the jth atom on the sth homological sites in the solid solution, and $\nu_{s,j,i}$ refers to the stoichiometric number of these sites occupied by the jth atom in one mole of the ith component. If we now adopt an intracrystalline standard state for which $\prod_s \prod_j a_{j,s}^{\nu_{s,j,i}} \rightarrow \prod_s \prod_j X_{j,s,i}^{\nu_{s,j,i}}$ as the mole fraction of the ith component of the solid solution approaches unity at any pressure and temperature, and specify an intercrystalline standard state calling for unit activity of the pure thermodynamic component in any specified state of substitutional order/disorder at a given pressure and temperature, $\mathbf{k}_i$ can be expressed as (Helgeson and Aagaard, 1984)

$$\mathbf{k}_i = \prod_s \prod_j X_{j,s,i}^{-\nu_{s,j,i}}, \quad (2)$$

where $X_{j,s,i}$ represents the mole fraction of the jth atom on the sth sites in one mole of the ith thermodynamic component. If, in addition, all of the atoms mix ideally on the respective sites represented by s so that $\prod_s \prod_j \lambda_{j,s}^{\nu_{s,j,i}} = 1$, Eq. (1) reduces to

$$a_i = \mathbf{k}_i \prod_s \prod_j X_{j,s}^{\nu_{s,j,i}}. \quad (3)$$

Note that only for a perfectly ordered component does $\mathbf{k}_i = 1$.

Activities of thermodynamic components corresponding in stoichiometry to pyrophyllite, margarite, paragonite, and muscovite (henceforth referred to as the pyrophyllite, margarite, paragonite, and muscovite components) computed from Eqs. (2) and (3) for the clay minerals discussed above are depicted in Figures 3 through 7. The specific statements of Eq. (3) are given by

$$a_{Al_2Si_4O_{10}(OH)_2} = \mathbf{k}_1(X_{V,A})(X_{Al,M(2)})^2(X_{Si,T})^4, \quad (4)$$

$$a_{CaAl_2(Al_2Si_2O_{10})(OH)_2} = \mathbf{k}_2(X_{Ca,A})(X_{Al,M(2)})^2(X_{Al,T_1})^2(X_{Si,T_2})^2, \quad (5)$$

$$a_{NaAl_2(AlSi_3O_{10})(OH)_2} = \mathbf{k}_3(X_{Na,A})(X_{Al,M(2)})^2(X_{Al,T})(X_{Si,T})^3, \quad (6)$$

and

$$a_{KAl_2(AlSi_3O_{10})(OH)_2} = \mathbf{k}_4(X_{K,A})(X_{Al,M(2)})^2(X_{Al,T})(X_{Si,T})^3, \quad (7)$$

where $X_{V,A}$ stands for the mole fraction of vacancies (V) on the A (exchange) sites, $X_{Ca,A}$, $X_{Na,A}$ and $X_{K,A}$ refer to the corresponding mole fractions of Ca, Na, and K on the A sites, $X_{Al,T}$, X_{Al,T_1}, $X_{Si,T}$, X_{Si,T_2}, and $X_{Al,M(2)}$ denote the mole fractions of Al and Si on the tetrahedral (T or T_1 and T_2) and M(2) octahedral sites, and $\mathbf{k}_1 = \mathbf{k}_2 = 1$ and $\mathbf{k}_3 = \mathbf{k}_4 = 9.4815$. The calculations were carried out for each of the 65 clay minerals by substituting in these equations the site occupancies cited above. For example, one of the Wyoming montmorillonites with the composition $(Na_{0.47}K_{0.015}Ca_{0.01})(Al_{1.54}Mg_{0.26}Fe^{2+}_{0.10}Fe^{3+}_{0.10})(Al_{0.14}Si_{3.86})O_{10}(OH)_2$ yields

$$a_{KAl_2(AlSi_3O_{10})(OH)_2} = 9.4815(0.015)(1.54/2)^2(0.14/4)(3.86/4)^3 = 0.00265 \quad (8)$$

and

$$a_{Al_2Si_4O_{10}(OH)_2} = 0.505(1.54/2)^2(3.86/4)^4 = 0.2597. \quad (9)$$

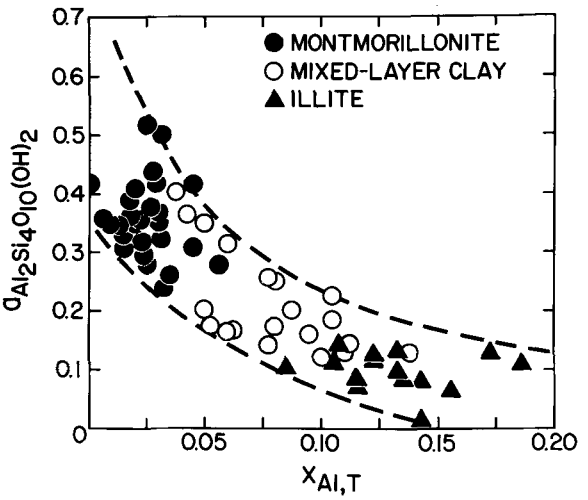

Figure 3. Correlation of the activities of the pyrophyllite component of the clay minerals shown in Figure 1 with the mole fraction of aluminum on the tetrahedral sites in the minerals (see text).

The dependence of the activities of the pyrophyllite and muscovite components of clay minerals on the mole fraction of aluminum on the tetrahedral sites in the minerals is depicted in Figures 3 and 4. Although the symbols representing the various clay minerals in these figures are somewhat scattered (owing to the dependence of the activities on other site occupancies), in both cases they fall within discrete ranges (delimited by the dashed lines) which trend toward increasing $a_{KAl_2(AlSi_3O_{10})(OH)_2}$ and decreasing $a_{Al_2Si_4O_{10}(OH)_2}$ with increasing $X_{Al,T}$.

It can be seen in the activity diagram shown in Figure 5 that the calculated activities of the pyrophyllite and muscovite components of montmorillonites, mixed-layer clays, and illites fall into discrete contiguous fields which exhibit a systematic trend as a function of log $a_{Al_2Si_4O_{10}(OH)_2}$ and log $a_{KAl_2(AlSi_3O_{10})(OH)_2}$. In contrast, no monotonic trend is apparent in the distribution of the fields shown in Figures 6 and 7, where log $a_{AlSi_4O_{10}(OH)_2}$

https://doi.org/10.1346/CCMN.1983.0310306 Published online by Cambridge University Press

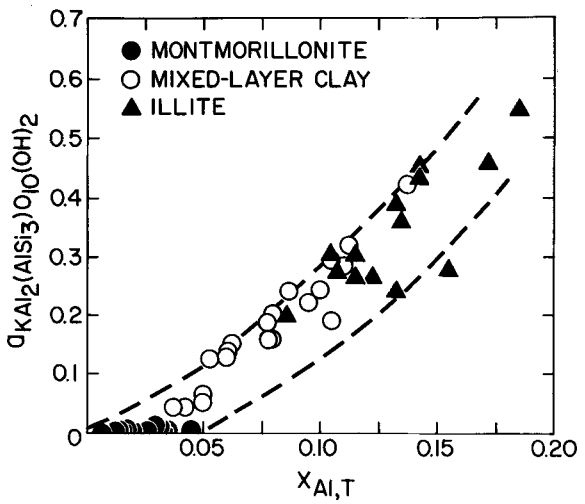

Figure 4. Correlation of the activities of the muscovite component of the clay minerals shown in Figure 1 with the mole fraction of aluminum on the tetrahedral sites in the minerals (see text).

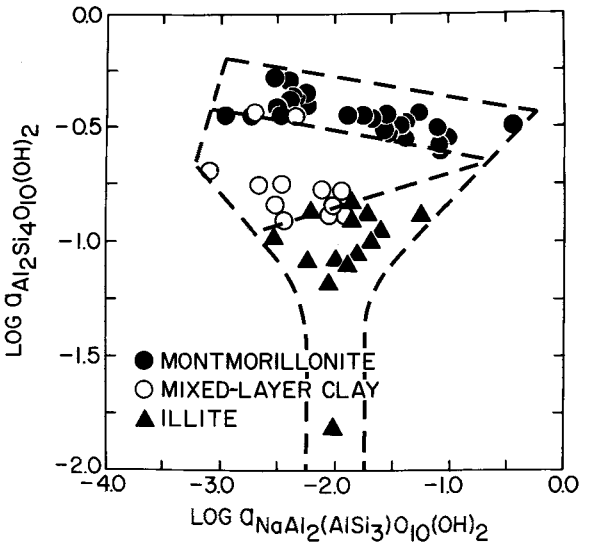

Figure 6. Correlation of the activities of the pyrophyllite and paragonite components of the clay minerals shown in Figures 1 and 2 computed from Eqs. (4) and (6) using site populations reported in the literature (see text).

in the clay minerals is shown as a function of log $a_{NaAl_2(AlSi_3O_{10})(OH)_2}$ and log $a_{CaAl_2(Al_2Si_2O_{10})(OH)_2}$. No mixed-layer clays appear in Figure 7 because the mixed-layer samples considered in the present study contain little or no Ca. Although dashed lines are used to delimit the fields corresponding to the various groups of clay minerals in Figures 5–7, the lines separating the fields are not meant to represent the coexistence of two phases. The boundaries of the fields merely designate limiting activities of the thermodynamic components of the solid solutions referred to as illite, montmorillonite, and illite/montmorillonite mixed-layer clay. In this context they are used below together with the systematic trend of the fields in Figure 5 to delimit the stability fields of the various clay minerals on logarithmic activity diagrams depicting phase relations in the system K_2O-Na_2O-CaO-MgO-FeO-Fe_2O_3-Al_2O_3-SiO_2-HCl-H_2O.

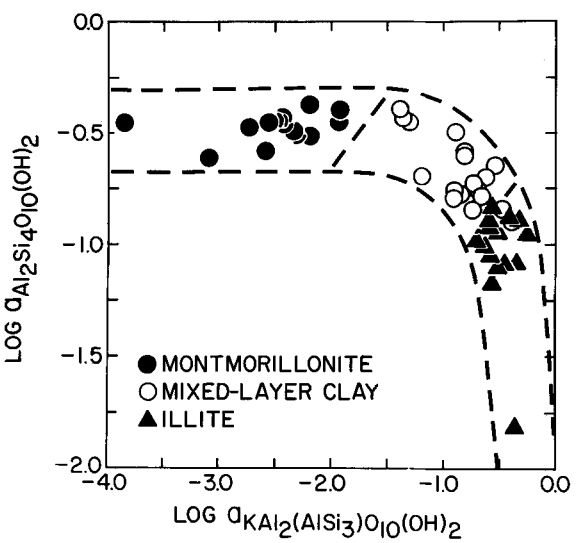

Figure 5. Correlation of the activities of the pyrophyllite and muscovite components of the clay minerals shown in Figures 1 and 2 computed from Eqs. (4) and (7) using site populations reported in the literature (see text). The dashed lines correspond to limits defined by the compositional data in Figure 1 for illites, montmorillonites, and mixed-layer clays.

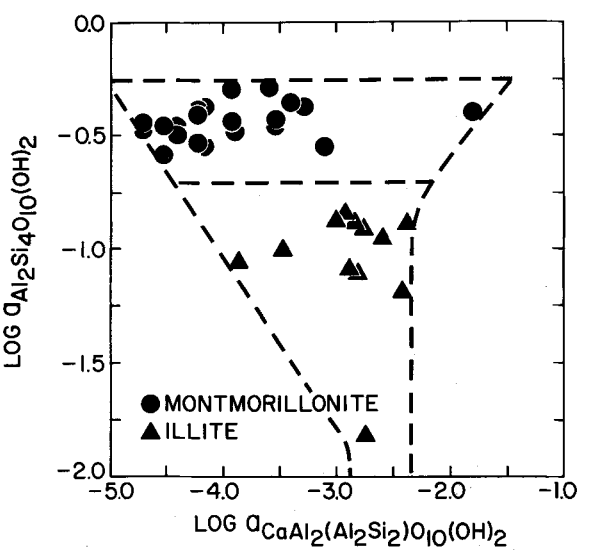

Figure 7. Correlation of the activities of the pyrophyllite and margarite components of the clay minerals shown in Figures 1 and 2 computed from Eqs. (4) and (5) using site populations reported in the literature (see text).

https://doi.org/10.1346/CCMN.1983.0310306 Published online by Cambridge University Press

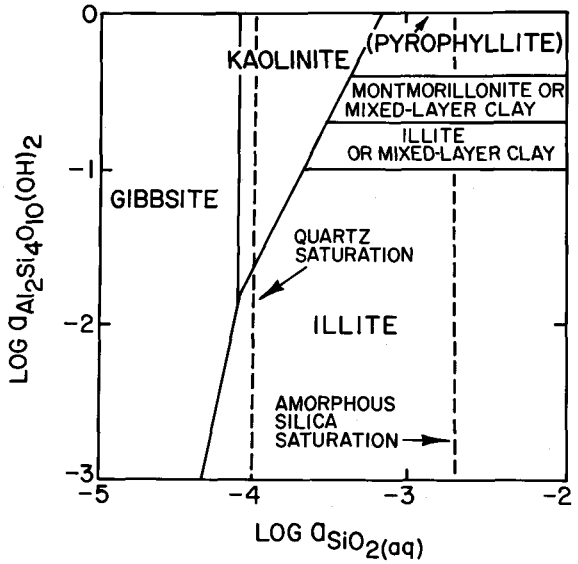

Figure 8. Logarithmic activity diagram depicting equilibrium phase relations among clay minerals and an aqueous solution at 25°C, 1 bar, and unit activity of H_2O (see text and caption of Figure 9).

ACTIVITY DIAGRAMS REPRESENTING EQUILIBRIUM AMONG CLAY MINERAL SOLID SOLUTIONS AND AN AQUEOUS PHASE

The activities of the thermodynamic components of clay minerals computed above, together with thermodynamic data for stoichiometric minerals and aqueous species taken from Helgeson *et al.* (1978) and Helgeson *et al.* (1981) were used to generate activity diagrams depicting stability fields of clay mineral solid solutions at 25°C, 1 bar, and unity activity of H_2O. The thermodynamic relations and procedure involved in constructing such diagrams have been discussed in detail by Garrels and Christ (1965), Helgeson *et al.* (1969), and others.

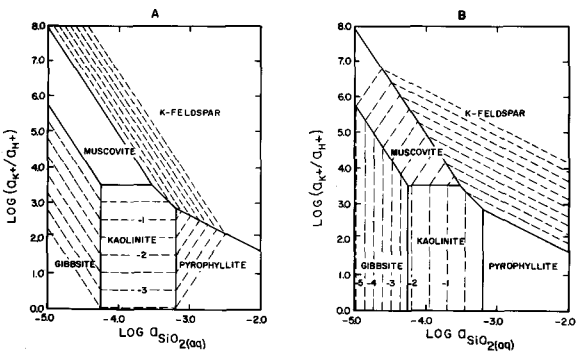

Figure 9. Logarithmic activity diagram depicting equilibrium phase relations among stoichiometric minerals in the system K_2O-Al_2O_3-SiO_2-HCl-H_2O at 25°C, 1 bar, and unit activity of H_2O generated from thermodynamic data given by Helgeson *et al.* (1978) and Helgeson *et al.* (1981). The dashed lines in diagrams A and B, respectively, correspond to contours of log $a_{KAl_2(AlSi_3O_{10})(OH)_2}$ and log $a_{Al_2Si_4O_{10}(OH)_2}$ in clay mineral solid solutions (see text).

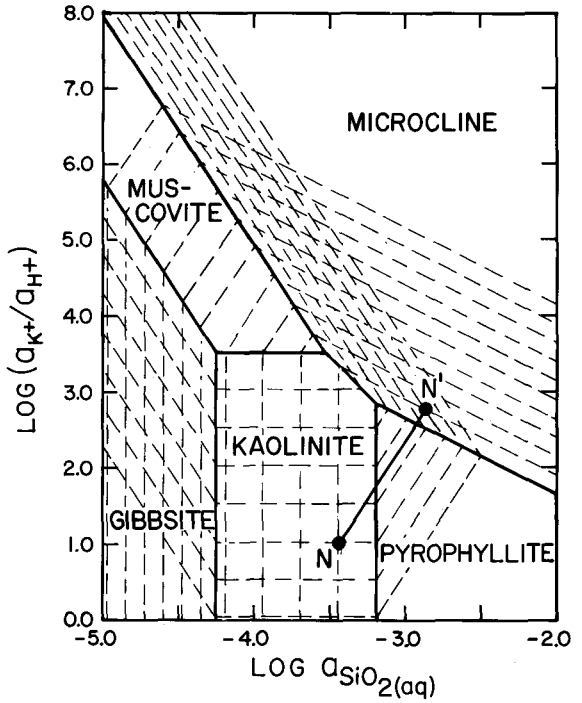

Figure 10. Composite activity diagram generated by superimposing diagrams A and B in Figure 9. Line NN′ is explained in the text.

Equilibrium phase relations among gibbsite, kaolinite, clay minerals, and an aqueous solution are depicted in Figure 8, which was generated using the dashed

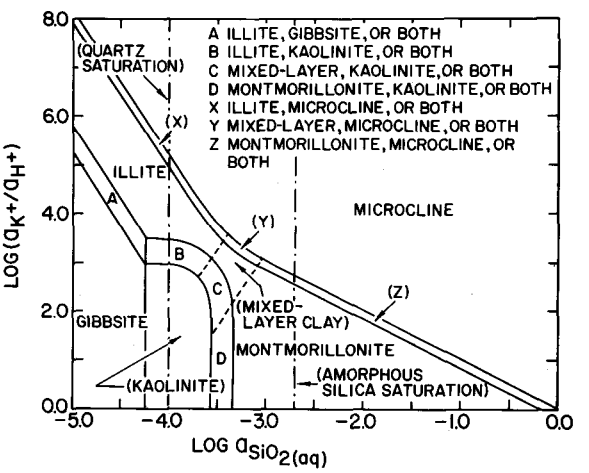

Figure 11. Logarithmic activity diagram depicting equilibrium phase relations among clay mineral solid solutions, stoichiometric minerals, and an aqueous solution at 25°C, 1 bar, and unit activity of H_2O. The positions of the stability field boundaries were computed from thermodynamic data taken from the sources cited in the caption of Figure 9 (see text).

https://doi.org/10.1346/CCMN.1983.0310306 Published online by Cambridge University Press

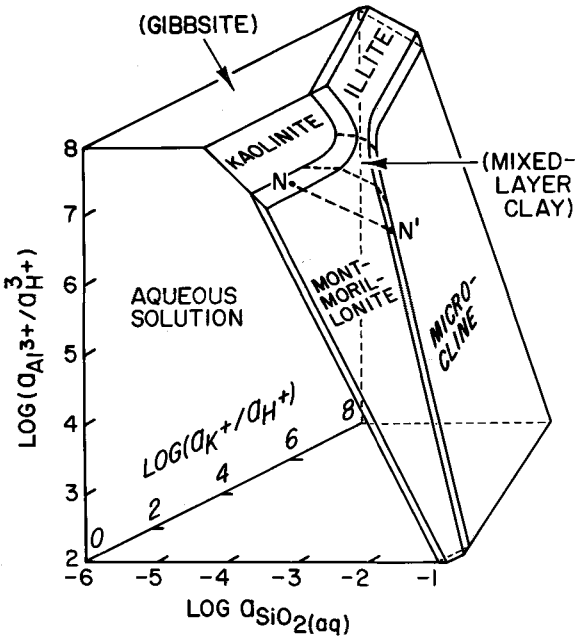

Figure 12. Three-dimensional logarithmic activity diagram for the system represented in two dimensions in Figure 11 (see text and caption of Figure 11).

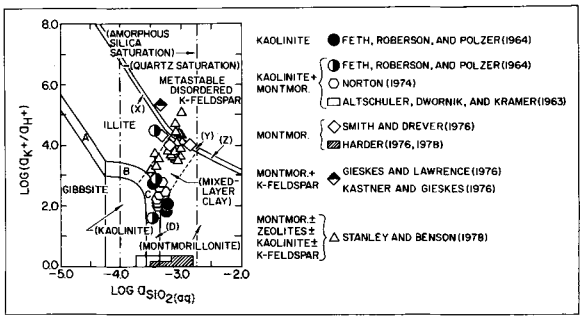

Figure 13. Correlation of $\log(a_{K^+}/a_{H^+})$ and $\log a_{SiO_2(aq)}$ in interstitial waters in soils and sediments (symbols) with equilibrium phase relations among clay minerals, metastable disordered K-feldspar, and an aqueous solution at 25°C, 1 bar, and unit activity of H_2O (see text). The stability field boundaries were generated using thermodynamic data taken from the sources cited in the caption of Figure 9.

boundaries in Figure 5 to distinguish among the various classes of clay minerals. The overlapping stability fields in Figure 8 arise from the fact that only one of the thermodynamic components of the clay minerals (the pyrophyllite component) is considered explicitly in the diagram. If both $a_{Al_2Si_4O_{10}(OH)_2}$ and $a_{KAl_2(AlSi_3O_{10})(OH)_2}$ are taken into account, the overlap in the stability fields of the clay minerals disappears.

Equilibrium among a clay mineral solid solution, an aqueous solution, and kaolinite can be represented by

$$Al_2Si_4O_{10}(OH)_2 + H_2O = Al_2Si_2O_5(OH)_4 + 2SiO_2(aq). \quad (10)$$

Hence, for unit activity of $Al_2Si_2O_5(OH)_4$ and H_2O,

$$\log a_{Al_2Si_4O_{10}(OH)_2} = 2 \log a_{SiO_2(aq)} - \log K \quad (11)$$

where K refers to the equilibrium constant for reaction (10). It thus follows that any change in the activity of the pyrophyllite component of clay minerals in equilibrium with kaolinite is proportional to the change in the activity of aqueous silica in the coexisting aqueous solution. Similarly, because for the same equilibrium state,

$$2KAl_2(AlSi_3O_{10})(OH)_2 + 2H^+ + 3H_2O = 3Al_2Si_2O_5(OH)_4 + 2K^+, \quad (12)$$

it follows that

$$\log a_{KAl_2(AlSi_3O_{10})(OH)_2} = \log(a_{K^+}/a_{H^+}) - 0.5 \log K, \quad (13)$$

which requires changes in the activity of the muscovite component of clay minerals to be proportional to corresponding changes in a_{K^+}/a_{H^+} in the aqueous phase. In all cases, the activities of the pyrophyllite, muscovite, and other components of the clay minerals can be cast in terms of the activities of $SiO_2(aq)$ and the cations in the coexisting aqueous phase. The geometric consequences of these relations are shown in the logarithmic activity diagrams depicted in Figures 9 and 10. Contours of $a_{KAl_2(AlSi_3O_{10})(OH)_2}$ and $a_{Al_2Si_4O_{10}(OH)_2}$, respectively, are shown in Figures 9A and 9B, which are superimposed in Figure 10. Line NN′ in Figure 10 designates $\log(a_{K^+}/a_{H^+})$ and $\log a_{SiO_2(aq)}$ in aqueous solutions coexisting with clay minerals in which $\log((a_{KAl_2(AlSi_3O_{10})(OH)_2})^2/(a_{Al_2Si_4O_{10}(OH)_2})^3)$ is constant, which is consistent with

$$2KAl_2(AlSi_3O_{10})(OH)_2 + 2H^+ + 6SiO_2(aq) = 3Al_2Si_4O_{10}(OH)_2 + 2K^+, \quad (14)$$

for which

$$\log(a_{K^+}/a_{H^+}) = \log a_{KAl_2(AlSi_3O_{10})(OH)_2} - 1.5 \log a_{Al_2Si_4O_{10}(OH)_2} - 3 \log a_{SiO_2(aq)} - 0.5 \log K, \quad (15)$$

where K refers to the equilibrium constant for reaction (14). Points N and N′, respectively, refer to a clay mineral with a particular composition in equilibrium with kaolinite (N) or K-feldspar (N′) and an aqueous phase, but intermediate points along line NN′ correspond only to equilibrium between an aqueous solution and clay minerals for which $(a_{KAl_2(AlSi_3O_{10})(OH)_2})^2/(a_{Al_2Si_4O_{10}(OH)_2})^3$ is constant.

The intersections of the two sets of contours in Figure 10 correspond to coordinates in Figure 5. Taking account of these intersections and the dashed lines in Figure 5 leads to the stability fields for the clay minerals shown in Figure 11, where it can be seen that kaolinite, gibbsite, or K-feldspar and a given type of clay mineral

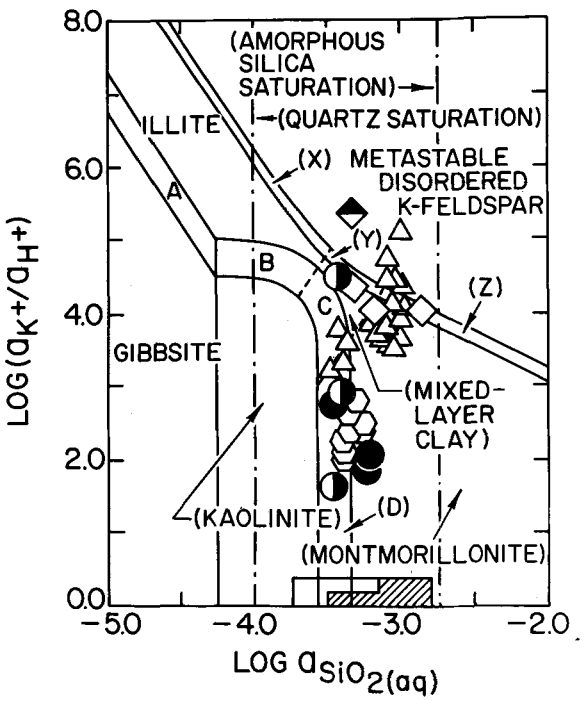

Figure 14. Correlation of log (a_{K^+}/a_{H^+}) and log $a_{SiO_2(aq)}$ in interstitial waters in soils and sediments (see Figure 13) with equilibrium phase relations among clay minerals, metastable disordered K-feldspar, and an aqueous solution at 25°C, 1 bar, and unit activity of H_2O. In contrast to Figures 9–13, the stability field boundaries shown above were generated with provision for a disordered $1M_d$ muscovite component of the clay minerals instead of the ordered $2M_1$ component used to calculate the phase relations shown in Figures 11–13 (see text and caption of Figure 13).

may coexist with an aqueous phase of variable composition in stability fields A, B, C, D, X, Y, or Z. The variability of the solution composition in these three-phase stability fields arises from two-dimensional representation of equilibrium in a multicomponent system. Note that the dashed lines in Figure 11, which separate the clay mineral designations, are not meant to imply discontinuities in the clay mineral solid solution series (see above).

Three dependent variables are specified implicitly by the equilibrium phase relations shown in Figure 11. These are $a_{Al_2Si_4O_{10}(OH)_2}$, $a_{KAl_2(AlSi_3O_{10})(OH)_2}$ and $a_{Al^{3+}}/a_{H^+}{}^3$. For example, values of $\log(a_{K^+}/a_{H^+})$ and $\log a_{SiO_2(aq)}$ corresponding to a given point in regions A, B, C, or D in Figure 11, together with Eqs. (11) and (13) specify corresponding values of $a_{Al_2Si_4O_{10}(OH)_2}$ and $a_{KAl_2(AlSi_3O_{10})(OH)_2}$. Note that it follows from

$$Al_2Si_4O_{10}(OH)_2 + 6H^+ = 2Al^{3+} + 4SiO_2(aq) + 4H_2O, \quad (16)$$

that $\log(a_{Al^{3+}}/a_{H^+}{}^3)$ is specified (for $a_{H_2O} = 1$) by

$$\log(a_{Al^{3+}}/a_{H^+}{}^3) = 0.5 \log a_{Al_2Si_4O_{10}(OH)_2} - 2 \log a_{SiO_2(aq)} - 0.5 \log K, \quad (17)$$

where K represents the equilibrium constant for reaction (16).

The relation of $\log(a_{Al^{3+}}/a_{H^+}{}^3)$ to $\log(a_{K^+}/a_{H^+})$ and $\log a_{SiO_2(aq)}$ in Figure 11 is depicted in Figure 12, where NN′ again represents a line of constant $(a_{KAl_2(AlSi_3O_{10})(OH)_2})^2/(a_{Al_2Si_4O_{10}(OH)_2})^3$. Note that in Figure 12 the clay minerals and the aqueous phase coexist in volumes of the three dimensional diagram, which is a consequence of the additional degrees of freedom (in the phase rule) represented by the activities of other components of the clay minerals.

The nonsystematic distribution of the data shown in Figures 6 and 7 leads to complicated and somewhat confusing activity diagrams with multiple overlapping fields in $\log(a_{Na^+}/a_{H^+})$ vs. $\log a_{SiO_2(aq)}$ and $\log(a_{Ca^{2+}}/a_{H^+}{}^2)$ vs. $\log a_{SiO_2(aq)}$ space. As a consequence, these diagrams have little practical value, which led to their omission from the present communication. Because the phase relations depicted in Figures 11 and 12 take into account implicitly all of the thermodynamic components of clay minerals, the activity diagrams shown in the figures suffice to describe equilibrium among these minerals, and aqueous solutions in a wide variety of geologic environments. The compositions of the clay minerals and coexisting aqueous solutions can be calculated numerically with the aid of equations summarized elsewhere (Helgeson and Aagaard, 1984).

Interpretation of phase relations

Values of $\log(a_{K^+}/a_{H^+})$ and $\log a_{SiO_2(aq)}$ computed from the compositions of interstitial waters reportedly coexisting with kaolinite and/or montmorillonite are shown in Figure 13, where it can be seen that most of the symbols fall in the mixed-layer clay stability field. Kinetic barriers may be responsible for much of the scatter (Dibble and Tiller, 1981), which could simply represent a myriad of metastable quasistatic states (Thorstenson and Plummer, 1977; Garrels and Wollast, 1978; Helgeson and Murphy, 1983). Although differences in sample temperatures of as much as 15°C cannot explain the apparent contradictions, the discrepancies could arise from several other sources. For example, the standard molal Gibbs free energy of formation of muscovite used to generate the activity diagram in Figure 13 represents the ordered $2M_1$ polytype, but most low-temperature authigenic illites correspond to metastable disordered $1M_d$ micas (Velde and Hower, 1963). No thermodynamic data are available for disordered $1M_d$ muscovite, but it would not be unreasonable in view of the thermodynamic consequences of substitutional disorder in alkali feldspars (Hovis, 1974; Thompson *et al.*, 1974; Helgeson *et al.*, 1978) to expect the standard molal Gibbs free energy of the disordered $1M_d$ polytype to be of the order of 2 kcal/mole less negative than that of the ordered $2M_1$ polytype. This would have the effect of expanding the stability fields of kaolinite and montmorillonite at the expense of those for illite and mixed-layer

clays, respectively, by 1.5 log units in $\log(a_{K^+}/a_{H^+})$. However, $\log(a_{K^+}/a_{H^+})$ corresponding to the coexistence of K-feldspar and illite would be lowered by 0.75 log units. As a consequence, the stability field of illite would be reduced considerably in size, as shown in Figure 14. Although Figure 14 is more consistent with the water compositions represented by the symbols in Figure 13, it can be argued that the small stability field of illite in Figure 14 is inconsistent with the common occurrence of the mineral in the geologic record. On the other hand, with the exception of high-temperature (100°C) data (Merino and Ransom, 1982), no compositions are available in the literature for waters that are known to coexist with illite.

The positions of the stability field boundaries shown in Figures 8 through 14 differ significantly from those of corresponding boundaries generated by Lippmann (1979), who used a set of thermodynamic data which is internally inconsistent. The coexistence of quartz and pyrophyllite in Lippmann's diagrams is incompatible with all of the pertinent experimental data cited by Helgeson *et al.* (1978). Although disordered K-feldspar is metastable with respect to microcline at 25°C and 1 bar, it was used to generate Figures 13 and 14 because most authigenic K-feldspars that are formed at low temperatures exhibit substitutional disorder (Kastner, 1971). The dearth of reliable thermodynamic data for phillipsite, clinoptilolite, and erionite precludes provision for these minerals in the diagrams. However, disordered K-feldspar can be regarded for the sake of the present discussion as a proxy for potassium zeolites, which are also almost certainly metastable with respect to ordered K-feldspar under near-surface conditions (Hay, 1977).

It can be deduced from Figures 13 and 14 that montmorillonite is incompatible with aqueous solutions that are in equilibrium with quartz at 25°C. This observation apparently applies to all temperatures below ~200°C. In contrast, both illite and K-feldspar may coexist with quartz. As a consequence, if local equilibrium is established between quartz and the interstitial waters in shales undergoing burial, montmorillonite would be expected to react with K-feldspar to produce illite and quartz. In other cases, montmorillonite may react with muscovite to form illite, quartz, and kaolinite (Hower *et al.*, 1976). In any event, regardless of whether mixed-layer clays are polyphase aggregates or solid solutions, the incompatibility of montmorillonite and quartz affords ample Gibbs free energy drive to promote diagenetic conversion of detrital smectite to illite with increasing burial.

The discrepancies between the compositions of waters reportedly coexisting with montmorillonite and the equilibrium values of $\log(a_{K^+}/a_{H^+})$ and $\log a_{SiO_{2(aq)}}$ corresponding to the montmorillonite stability field in Figure 13 could be a consequence of the metastable persistence of montmorillonite in geologic systems. It may well be that the outer surfaces of the montmorillonite grains in contact with the waters shown in Figures 13 and 14 have been converted to mixed layer clays in local equilibrium with the aqueous phase, but the amount formed is so minor that it escaped attention (Berner, 1971). *It should be emphasized in this regard that the water compositions shown in these figures are no more compatible with the behavior of mixed-layer clays corresponding to polyphase aggregates than they are with the solid solution model represented by the stability fields in the diagrams.*

It can be seen in Figures 13 and 14 that the bulk of the data reported by Norton (1974) and Feth *et al.* (1964) are consistent with kaolinite coexisting with montmorillonite or mixed-layer clays. In contrast, the water analyses reported by Stanley and Benson (1979) are compatible with K-feldspar coexisting with montmorillonite or mixed-layer clays. These associations are in general agreement with the geologic settings represented by the samples. For example, Stanley and Benson's (1979) analyses are of waters associated with alteration of feldspar to montmorillonite and/or mixed-layer clays.

CONCLUDING REMARKS

Despite the fact that assuming ideal mixing of atoms on homological sites in clay minerals takes no account of immiscibility or changes in solvation of the interlayer cations (Garrels and Tardy, 1982) as a function of composition, the equations and calculations summarized above afford reasonable approximation of observed phase relations among clay minerals and aqueous solutions in geologic systems. It thus appears that higher-order mixing models such as the regular solution approach taken by Garrels and Christ (1965), Truesdell and Christ (1968), and Stoessell (1979, 1981) are unnecessary to achieve quasi-agreement between calculated and observed mineral and fluid compositions. However, because of the scatter in the data, none of these compositions is definitive with respect to whether mixed-layer clays behave as solid solutions or polyphase aggregates in geochemical processes.

ACKNOWLEDGMENTS

The present communication represents part of the senior author's Ph.D. dissertation at the University of California, Berkeley. The research was supported by the Norwegian Research Council for Science and the Humanities, a Fullbright-Hays travel grant, and National Science Foundation grants EAR 74-14280 and EAR 77-14492. We are indebted to G. Flowers, D. Bird, J. Walther, P. Behrman, J. Delany, W. McKenzie, M. Moore, E. Shock, M. Lee, J. Hampel, B. Rosenbaum, D. Maskell, and J. Bossart for discussion and technical assistance. Thanks are also due R. Reynolds, D. Eberl, E. Merino, J. Grover, and R. Garrels for constructive reviews of the manuscript. Finally, we would like to acknowledge the help of L. Benson in the early stages of the study.

REFERENCES

Altschuler, Z. S., Dwornik, E. J., and Kramer, H. (1963) Transformation of montmorillonite to kaolinite during weathering: *Science* **141,** 148–152.

Bailey, S. W. (1975) Cation ordering and pseudosymmetry in layer silicates: *Amer. Mineral.* **60,** 175–187.

Berner, R. A. (1971) *Principles of Chemical Sedimentology:* McGraw Hill, New York, 240 pp.

Brown, G. and Norrish, K. (1952) Hydrous micas: *Min. Mag.* **29,** 929–932.

Burnham, C. W. and Radoslovich, E. W. (1964) Crystal structures of coexisting muscovite and paragonite: *Carnegie Inst. Wash. Yearbook* **63,** 232–236.

Coey, J. M. D. (1975) The clay minerals; use of Mössbauer effect to characterize them and study their transformations: *Proc. Intern. Conf. Mössbauer Spectr., Cracow.*

Dibble, W. E., Jr. and Tiller, W. A. (1981) Kinetic model of zeolite paragenesis in tuffaceous sediments: *Clays & Clay Minerals* **29,** 323–330.

Ericsson, T., Wappling, R., and Punakivi, K. (1977) Mössbauer spectroscopy applied to clay and related minerals: *Geol. For. Forhandlingar* **99,** 229–244.

Feth, J. H., Roberson, C. E., and Polzer, W. L. (1964) Sources of mineral constituents in water from granitic rocks, Sierra Nevada, California and Nevada: *U.S. Geol. Surv. Water-Supp. Pap.* **1535-i,** 70 pp.

Garrels, R. M. and Christ, C. L. (1965) *Solutions, Minerals and Equilibria:* Harper and Row, New York, 450 pp.

Garrels, R. M. and Tardy, Y. (1982) Born-Haber cycles for interlayer cations of micas: in *Proc. 7th Int. Clay Conf., Bologna and Pavia, 1981,* H. van Olphen and F. Veniale, eds., Elsevier, Amsterdam, 423–440.

Garrels, R. M. and Wollast, R. (1978) Discussion: *Amer. J. Sci.* **278,** 1469–1474.

Gatineau, L. (1964) Structure réele de la muscovite. Répartition des substitutions isomorphes: *Bull. Soc. Fr. Minéral. Crystallogr.* **87,** 321–355.

Gieskes, J. M. and Lawrence, J. R. (1976) Interstitial water studies, Leg 35: in *Initial Reports of the Deep Sea Drilling Project 35,* C. D. Hollister, ed., Washington, D.C., U.S. Government Printing Office, 407–424.

Guggenheim, S. and Bailey, S. W. (1975) Refinement of the margarite structure in subgroup symmetry: *Amer. Mineral.* **60,** 1023–1029.

Harder, H. (1976) Nontronite synthesis at low temperatures: *Chem. Geol.* **18,** 169–180.

Harder, H. (1977) Clay mineral formation under lateritic weathering conditions: *Clay Miner.* **12,** 281–288.

Hay, R. L. (1977) Geology of zeolites in sedimentary rocks: in *Mineralogy and Geology of Natural Zeolites,* F. A. Mumpton, ed., Min. Soc. Amer. Short Course Notes **4,** 53–64.

Helgeson, H. C. (1969) Thermodynamics of hydrothermal systems at elevated temperatures and pressures: *Amer. J. Sci.* **267,** 724–804.

Helgeson, H. C. and Aagaard, P. (1984) Activity/composition relations among silicates and aqueous solutions. I. Thermodynamics of intrasite mixing and substitutional order/disorder in minerals: *Amer. J. Sci.* **284** (in press).

Helgeson, H. C., Brown, T. H., and Leeper, R. H. (1969) *Handbook of Theoretical Activity Diagrams Depicting Chemical Equilibria in Geologic Systems Involving an Aqueous Phase at One Atm. and 0°C to 300°C:* Freeman, Cooper & Co., San Francisco, 253 pp.

Helgeson, H. C., Delany, J. M., Nesbitt, H. W., and Bird, D. K. (1978) Summary and critique of the thermodynamic properties of rock forming minerals: *Amer. J. Sci.* **278-A,** 229 pp.

Helgeson, H. C., Kirkham, D. H., and Flowers, G. C. (1981) Theoretical prediction of the thermodynamic behavior of aqueous electrolytes at high pressures and temperatures. IV. Calculation of activity coefficients, osmotic coefficients, and apparent molal and standard and relative partial molal properties of 5 kb and 600°C: *Amer. J. Sci.* **281,** 1249–1516.

Helgeson, H. C. and MacKenzie, F. T. (1970) Silicate-sea water equilibria in the ocean system: *Deep-Sea Res.* **17,** 877–892.

Helgeson, H. C. and Murphy, W. M. (1983) Calculation of mass transfer among minerals and aqueous solutions as a function of time and surface area in geochemical processes. I. Computational approach: *Math. Geol.* **15,** 109–130.

Hovis, G. L. (1974) A solution calorimetric and X-ray investigation of Al-Si distribution in monoclinic potassium feldspars: in *The Feldspars,* W. S. MacKenzie and J. Zussman, eds., Crane, Russak, and Co., Inc., New York, 114–144.

Hower, J. and Mowatt, T. C. (1966) The mineralogy of illites and mixed-layer illite/montmorillonites: *Amer. Mineral.* **51,** 825–854.

Hower, J., Eslinger, E. V., Hower, M. E., and Perry, E. A. (1976) Mechanism of burial metamorphism of argillaceous sediment: 1. Mineralogical and chemical evidence: *Geol. Soc. Amer. Bull.* **87,** 725–737.

Kastner, M. (1971) Authigenic feldspars in carbonate rocks: *Amer. Mineral.* **56,** 1403–1443.

Kastner, M. and Gieskes, J. M. (1976) Interstitial water profiles and sites of diagenetic reactions, Leg 35, DSDP, Bellingshausen Abyss/Plain: *Earth Plan. Sci. Lett.* **33,** 11–20.

Kittrick, J. A. (1971) Stability of montmorillonites: I. Belle Fourche and Clay Spur montmorillonites: *Soil Sci. Soc. Amer. Proc.* **35,** 140–145.

Lippmann, F. (1979) Stability diagrams involving clay minerals: in *Proc. 8th Conf. on Clay Mineralogy and Petrology, Teplice,* J. Konta, ed., Univ. Karlova, Praha, 153–171.

Mattigod, S. V. and Sposito, G. (1978) Improved method for estimating the standard free energies of formation ($\delta G_{f,298.15}$) of smectites: *Geochim. Cosmochim. Acta* **42,** 1753–1762.

Merino, E. and Ransom, B. (1982) Free energies of formation of illite solid solutions and their compositional dependence: *Clays & Clay Minerals* **30,** 29–39.

Norton, D. (1974) Chemical mass transfer in the Rio Tanama system, west-central Puerto Rico: *Geochim. Cosmochim. Acta* **38,** 267–277.

Nriagu, J. O. (1975) Thermochemical approximations for clay minerals: *Amer. Mineral.* **60,** 834–839.

Page, R. (1977) Alteration-mineralization history of the Butte, Montana, ore deposit, and transmission electron microscopy of phyllosilicate alteration phases: Ph.D. thesis, University of California, Berkeley, 226 pp.

Perry, E. and Hower, J. (1970) Burial diagenesis in Gulf Coast pelitic sediments: *Clays & Clay Minerals* **18,** 165–177.

Reynolds, R. C., Jr. and Hower, J. (1970) The nature of interlayering in mixed-layer illite-montmorillonites: *Clays & Clay Minerals* **18,** 25–36.

Ross, C. S. and Hendricks, S. B. (1945) Minerals of the montmorillonite group: *U.S. Geol. Surv. Prof. Pap.* **205-B,** 23–79.

Routson, R. C. and Kittrick, J. A. (1971) Illite solubility: *Soil Sci. Soc. Amer. Proc.* **35,** 714–718.

Schultz, L. G. (1969) Lithium and potassium absorption, dehydroxylation temperature, and structural water 3 content of aluminous smectites: *Clays & Clay Minerals* **17,** 115–149.

Smith, C. L. and Drever, J. I. (1976) Controls on the chemistry of springs at Teels Marsh, Mineral County, Nevada: *Geochim. Cosmochim. Acta* **40,** 1081–1094.

Smith, J. V. and Yoder, H. S., Jr. (1956) Experimental and theoretical studies of the mica polymorphs: *Min. Mag.* **31,** 209–235.

Stanley, K. O. and Benson, L. V. (1979) Early diagenesis of High Plaines Tertiary vitric and arkosic sandstone, Wyoming and Nebraska: *Soc. Econ. Pal. Mineral., Spec. Publ.* **26,** 401–423.

Stoessell, R. K. (1979) A regular solution site-mixing model for illites. *Geochim. Cosmochim. Acta* **43,** 1151–1159.

Stoessell, R. K. (1981) Refinements in a site-mixing model for illites: local electrostatic balance and the quasi-chemical approximation: *Geochim. Cosmochim. Acta* **45,** 1733–1741.

Sudo, T., Shimoda, S., Yotsumoto, H., and Saburo, A. (1981) *Electron Micrographs of Clay Minerals:* Elsevier, Amsterdam, 203 pp.

Tardy, Y. and Fritz, B. (1981) An ideal solution model for calculating solubility of clay minerals: *Clay Miner.* **16,** 361–373.

Tardy, Y. and Garrels, R. M. (1974) A method of estimating the Gibbs energies of formation of layer silicates: *Geochim. Cosmochim. Acta* **38,** 1101–1116.

Thompson, J. B., Jr., Waldbaum, D. R., and Hovis, G. L. (1974) Thermodynamic properties related to ordering in end-member feldspars: in *The Feldspars,* W. S. MacKenzie and J. Zussman, eds., Crane, Russak and Co., Inc., New York, 218–248.

Thorstenson, D. C. and Plummer, L. N. (1977) Equilibrium criteria for two-component solids reacting with fixed composition in an aqueous phase—Example: The magnesian calcites: *Amer. J. Sci.* **277,** 1203–1223.

Truesdell, A. H. and Christ, C. L. (1968) Cation exchange in clays interpreted by regular solution theory: *Amer. J. Sci.* **266,** 402–412.

Velde, B. (1977) *Clays and Clay Minerals in Natural and Synthetic Systems:* Elsevier, Amsterdam, 218 pp.

Velde, B. and Hower, J. (1963) Petrological significance of illite polymorphism in Paleozoic sedimentary rocks: *Amer. Mineral.* **48,** 1239–1254.

Weaver, C. E. and Pollard, L. D. (1973) *The Chemistry of Clay Minerals:* Elsevier, Amsterdam, 213 pp.

Welton, J. E. (1980) Petrology and diagenesis of the Early Miocene Skooner Gulch and Gallaway Formations, Point Arena, California. M.S. thesis, University of Southern California, 123 pp.

Wilson, M. D. and Pittman, E. P. (1977) Authigenic clays in sandstones: recognition and influence on reservoir properties and paleoenvironmental analysis: *J. Sed. Petrol.* **47,** 3–31.

Zen, E. A. (1962) Problem of the thermodynamic status of the mixed layer minerals: *Geochim. Cosmochim. Acta* **26,** 1055–1067.

Zvyagin, B. B. (1967) *Electron-Diffraction Analysis of Clay Mineral Structures:* Plenum Press, New York, 364 pp.

(Received 1 October 1982; accepted 5 December 1982)

Резюме—Рассаитывались активности термодинамических компонентов глинистых минералов, соответствующих по составу пирофиллиту, мусковиту, парагониту и маргариту. Расчет был проведен на основании опубликованных данных химических анализов, предполагая идеальную смесь атомов в гомологических местах минералов. Полученные величины активностей использовались для определения полей стабильности смектитов, иллитов, и переслаивающихся глин на логаритмических диаграммах активностей, представляющих равновесие между минералами и водным раствором при температуре 25°C и давлении 1 бар. Сравнительный анализ указывает на то, что этот подход хорошо описывает состав минералов и воды в геологических системах. [E.G.]

Resümee—Die Aktivitäten der thermodynamischen Komponenten von Tonmineralen, die in ihrer Zusammensetzung Pyrophyllit, Muskovit, Paragonit, und Margarit entsprechen, wurden aus chemischen Analysen, die in der Literatur angegeben sind, mittels Computer berechnet, wobei eine ideale Mischung von Atomen auf homologen Plätzen in den Mineralen angenommen wird. Diese Aktivitäten wurden dann verwendet, um die Stabilitätsbereiche von Smektiten, Illiten und Wechsellagerungstonen in logarithmischen Diagrammen aufzustellen, die Gleichgewicht zwischen den Mineralen und den wässrigen Lösungen bei 25°C und 1 Bar darstellen. Vergleichende Analysen deuten darauf hin, daß dieses Vorgehen zu einer guten Annäherung an die Mineral- und Wasserzusammensetzung in geologischen Systemen führt. [U.W.]

Résumé—Les activités des composés thermodynamiques de minéraux argileux correspondant en composition à la pyrophyllite, muscovite, paragonite, et margarite ont été computés à partir d'analyses chimiques rapportées dans la littérature, supposant un mélange idéal d'atomes sur des sites homologues dans les minéraux. Ces activités ont alors été utilisées pour générer des champs d'équilibre pour des smectites, illites et argiles à couches mélangées sur des diagrammes d'activité logarithmique représentant l'équilibre entre les minéraux et des solutions aqueuses à 25°C et 1 bar. L'analyse comparative indique que cette approche permet une approximation proche des compositions minérales et aqueuses dans des systèmes géologiques. [D.J.]